Saudi Pharmaceutical Journal 29 (2021) 1102–1111

Contents lists available at ScienceDirect

Saudi Pharmaceutical Journal

journal homepage: www.sciencedirect.com

Original article

New terpenic and phenolic compounds from *Suaeda monoica* reverse oxidative and apoptotic damages in human endothelial cells

Mohammad K. Parvez [a,*], Mohammed S. Al-Dosari [a], Md. Tabish Rehman [a], Mohammed F. Alajmi [a], Ali S. Alqahtani [a,b], Mansour S. AlSaid [a,b]

[a] Department of Pharmacognosy, College of Pharmacy, King Saud University, Riyadh, Saudi Arabia
[b] Medicinal, Aromatic and Poisonous Plants Research Center, College of Pharmacy, King Saud University, Riyadh, Saudi Arabia

ARTICLE INFO

Article history:
Received 1 March 2021
Accepted 1 August 2021
Available online 9 August 2021

Keywords:
Suaeda monoica
Terpenes
Methylglyoxal
Dichlorofluorescin
Endothelial cells
Apoptosis

ABSTRACT

Elevation in hyperglycemia-associated methylglyoxal level can trigger vascular endothelial cells oxidative stress and apoptosis. The present work assesses the cell proliferative, anti-oxidative and anti-apoptotic potential of *Suaeda monoica* derived four new terpenes: a norsesquaterpenol (normonisesquaterpenol), a monocyclic triterpenoid (suaedanortriterpene dione), an aromatic monoterpenic ester and a labdane-type norditerpenic xyloside as well as two new phenols: an alkylated β-naphthol and a β-methoxy naphthalene in cultured human umbilical vein endothelial cells (HUVEC). Of these, suaedanortriterpenedione (53.7%), normonisesquaterpenol (51.4%) and norditerpenic xyloside (48%) showed the most promising cell proliferative activities compared to others. Moreover, normonisesquaterpenol, norditerpenic xyloside and suaedanortriterpenedione efficiently reversed the oxidative and apoptotic cell damage via downregulation of capase-3/7 by 44.3%, 42.2% and 39.4%, respectively against dichlorofluorescin, whereas by 46.2%, 43.5% and 42.5%, respectively against methylglyoxal. Aminoguanidine, the reference drug inhibited caspase-3/7 activity by 56.2% and 54.7% through attenuation of dichlorofluorescin and methylglyoxal, respectively. Further *in silico* molecular docking analysis revealed formation of stable complexes between the tested compounds and caspase-3/7. Conclusively, we for the first time demonstrate the growth stimulatory, anti-oxidative and anti-apoptotic salutations of *S. monoica* derived novel compounds in human endothelial cells. This warrants their further assessment as vascular cell protective and rejuvenating therapeutics, especially in hyperglycemic conditions.

1. Introduction

In recent times, several plant extracts and their bioactive constituents have shown promising growth stimulatory or cytoprotective potential (Kong et al., 2004; Kim et al., 2013; Arbab et al., 2016; Parvez et al., 2018) warranting their further exploitation as anti-oxidative, anti-inflammatory or tissue-rejuvenating agents. The mangrove herb *Suaeda monoica* J. F. Gmel (Chenopodiaceae) is traditionally used to treat sore throat, rheumatism, asthma, snake-bites, skin disease, ulcer, hepatotoxicity, and microbial infections (Kathiresan and Ramanathan, 1997; Muthazhagan et al., 2014; Lakshmi and Narsimha Rao, 2013). In addition, its flavonoids, saponins, alkaloids, polyphenols, resins, tannins, coumarins, cardiac glycosides, and fatty acids are characterized as therapeutic phytoconstituents (Kokpal et al., 1990; Lakshmanan et al., 2013; Muthazhagan et al., 2014). Recently, we have reported isolation and preliminary bioactivity of *S. monoica* derived four new terpenes: a norsesquaterpenol (normonisesquaterpenol), a monocyclic triterpenoid (suaedanortriterpene dione), an aromatic monoterpenic ester, an unknown labdane-type norditerpenic xyloside as well as two new phenols: an alkylated β-naphthol and a β-methoxy naphthalene derivative (AlSaid et al., 2017; Siddiqui et al., 2020). Notably, a novel pentacyclic triterpenedione from *Picea jezoensis* with unknown bioactivity has been previously reported (Tanaka et al., 1997).

The vascular endothelial cells, the inner layer of blood vessel is crucial in modulating vascular function and homeostasis (Choy

* Corresponding author at: Department of Pharmacognosy, College of Pharmacy, King Saud University, Riyadh 11451, Saudi Arabia.
E-mail address: mohkhalid@ksu.edu.sa (M.K. Parvez).
Peer review under responsibility of King Saud University.

Production and hosting by Elsevier

https://doi.org/10.1016/j.jsps.2021.08.007
1319-0164/

et al., 2001). In conditions with hyperglycemia, retardation of endothelial cells proliferation or apoptosis often leads to diabetic microvascular lesions and cardiovascular complications. Methylglyoxal (MGO) is a highly reactive aldehyde that is produced as a byproduct of several metabolic pathways, including lipid peroxidation (Thornalley and Rabbani, 2014). Also, it is a major precursor of advanced glycation end products implicated in the development of type-2 diabetic complications (Vander Jagt and Hunsaker, 2003) as well oxidative stress and apoptosis in endothelial cells (Bourajjaj et al., 2003; Thornalley and Rabbani, 2014). In addition, high level of MGO is demonstrated to cause *in vitro* hyperglycemia and oxidative damages in human umbilical vein endothelial cells (Bourajjaj et al., 2003). In endothelial cells, MGO-induced oxidative stress and apoptosis is suggested mainly through the generation of reactive-oxygen species (Phalitakul et al., 2013; Figarola et al., 2014; Kim et al., 2004).

Dichlorofluorescin (DCF), is generally used to measure cellular oxidative stress as a result of H_2O_2-dependent reactions, including cytochrome *C* and Fe^{2+} (Royall and Ischiropoulos, 1993; Carter et al., 1994; LeBel et al., 1992). In line with this, we have recently reported DCFH and MGO induced oxidative stress and apoptosis in a variety of cells, including HUVEC (Arbab et al., 2016; Shahat et al., 2017; Parvez et al., 2018; Parvez et al., 2019; Alqahtani et al., 2019; Parvez et al., 2020). In this report, we have investigated the cytoprotective potential of *S. monoica* derived six novel compounds against MGO and DCFH induced oxidative and apoptotic damages in cultured HUVEC cells.

2. Materials and methods

2.1. Extraction, isolation and structure elucidation of the compounds

The extraction and isolation of six novel compounds: a norsesquaterpenol (normonisesquaterpenol), a monocyclic triterpenoid (suaedanortriterpenedione), an aromatic monoterpenic ester, an unknown labdane-type norditerpenic xyloside, an alkylated β-naphthol and a β-methoxy naphthalene derivative from the aerial parts of *S. monoica* (voucher specimen no. 15135), including their structure elucidations (Fig. 1) have been previously reported by us (AlSaid et al., 2017; Siddiqui et al., 2020).

2.2. Cell culture

Human umbilical vein epithelial cells (HUVEC 16549; ATCC, USA) were maintained in DMEM-Glutmax medium (Gibco, USA), supplemented with 10% fetal calf serum (Gibco, USA) and 1x penicillin–streptomycin mix (Invitrogen, USA) at 37 °C with 5% CO_2 supply. HUVEC cells ($0.5x10^5$/100 µl/well) were seeded in a 96-well flat-bottom plate (Becton-Dickinson Labware, USA) and grown overnight for all experiments.

2.3. Natural compounds and drugs preparations

The *S. monoica* derived norsesquaterpenol (NSQ), suaedanortriterpenedione (SND), aromatic monoterpenic ester (AES), norditerpenic xyloside (NDX), alkylated β-naphthol (ABN) and β-methoxy naphthalene (BMN) were first dissolved in 50 µl dimethyl sulfoxide (DMSO, Sigma-Alderich, Germany) and reconstituted in culture media (1 mg/ml, each). Based on our previously assessed non-toxic concentrations on liver cancer cells (AlSaid et al., 2017; Siddiqui et al., 2020), only three working doses (50, 25 and 12.5 µg/ml; DMSO < 0.5% final) were further prepared in culture media. Likewise, DCF and MGO (Sigma-Alderich, Germany) were prepared to be used as inducers of oxidative and apoptotic cell damage, whereas aminoguanidine (AG; Sigma-Alderich, Germany) served as anti-apoptotic agent (positive control).

2.4. Microscopy

Visual monitoring of the treated cells for any morphological changes, cytotoxicity or proliferation cells was made under an inverted microscope (Optica, 40x and 100x).

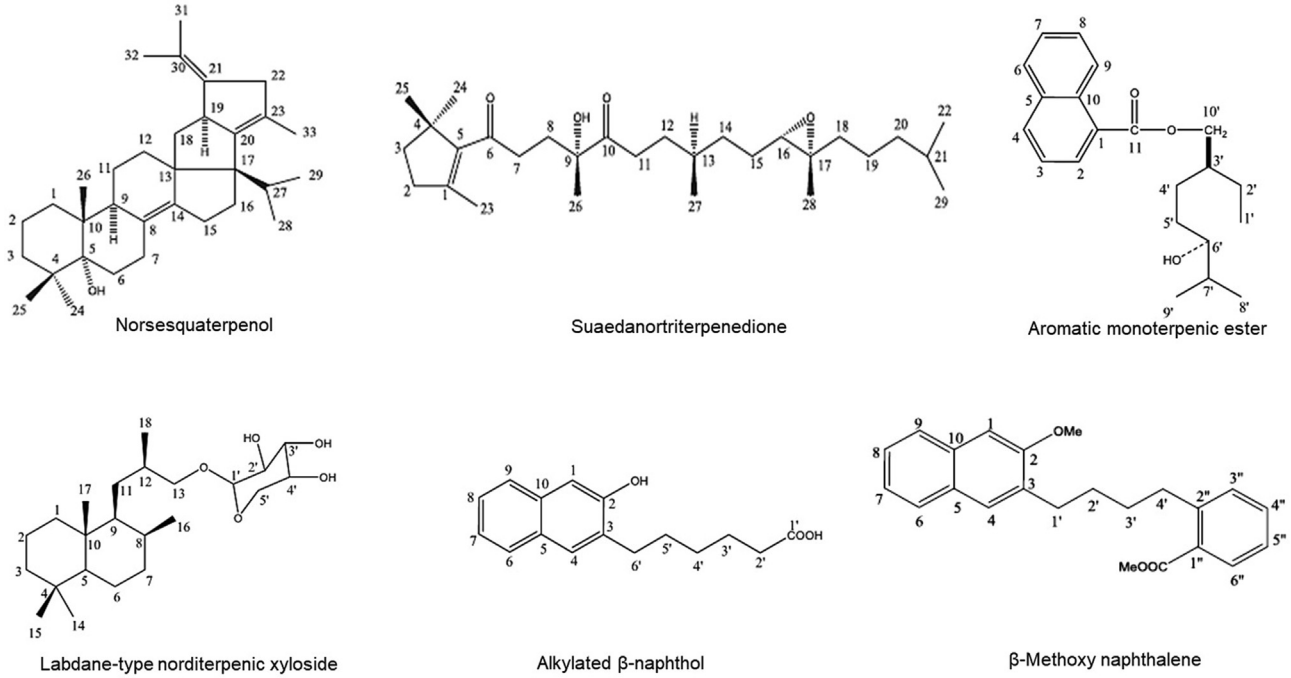

Fig. 1. Chemical structure of *Suaeda monoica* derived new terpenic and phenolic compounds: normonisesquaterpenol, suaedanortriterpenedione, aromatic monoterpenic ester, norditerpenic xyloside, alkylated β-naphthol and β-methoxy naphthalene.

2.5. Cell proliferation assay of S. Monoica derived compounds

The *S. monoica* derived compounds: NSQ, SND, AES, NDX, ABN, BMN were tested for their cell proliferative or growth stimulatory activities in cultured HUVEC cells. Cells were treated with the different doses of the compounds, including untreated control (0.5% DMSO) for 3 days. MTT assay (TACS MTT Cell Proliferation Assay Kit, Tervigen, USA) was performed as per the kit's manual. Briefly, the MTT reagent (10 µl/well) was added and incubated in dark for about 4 h at room temperature (RT) until purple color appeared. Further the detergent solution (100 µl/well) was added and the cells were incubated for another 1.5 h at 37 °C. The optical density (OD; λ = 570) was measured (Microplate reader ELx800; BioTek, USA) and data was analyzed by non-linear regression (Excel software 2010; Microsoft, USA) to determine the cell proliferation in relation to the untreated control [%Cell proliferation = (OD_{sample}- − OD_{blank}/$OD_{control}$ − OD_{blank}) x100]. All samples were tested in triplicate and repeated.

2.6. Assessment of anti-oxidative and cytoprotective activity of S. Monoica derived compounds

HUVEC cell grown in a 96-well plate were treated with DCF (IC_{50}: 32.5 µg/ml) as described elsewhere (Parvez et al., 2020) plus a dose of NSQ, SND, AES, NDX, ABN or BMN. DCFH and DMSO served as negative and untreated control, respectively. The culture was incubated for 3 days at 37 °C and MTT assay was performed to determine the cell survival (%) as above. All samples were tested in triplicate and repeated.

2.7. Anti-apoptotic activity assay of S. Monoica derived compounds

HUVEC cells grown in a 96-well plate were treated with MGO (0.5 mM) as described elsewhere (Alqahtani et al., 2019) plus a dose of NSQ, SND, AES, NDX, ABN or BMN. MGO and AG (0.05 mM; Alqahtani et al., 2019) served as negative and positive control, respectively. The treated cells were incubated for 3 days and MTT assay was performed to determine the cell survival (%) as above. All samples were tested in triplicate and repeated.

2.8. Assessment of caspase-3/7 modulating activity of S. Monoica derived compounds

Based on the promising anti-oxidative and anti-apoptotic activities, an optimal dose (25 µg/ml) of the compounds was tested for cellular caspase-3/7 activation in HUVEC cells in 96-well plates (Set-I: DCF treated and Set-II: MGO treated). Day 3 post-incubation, cellular caspase expressions were measured (Apo-ONE-cas3/7 assay kit; Promega, USA) as per the kit's manual., Briefly, 100 µl of caspase-3/7 reagent was added to each well, mixed by gentle rocking and incubated in dark for ~ 6 h at RT. Caspase reagent plus culture medium served as blank while reagent plus DMSO treated cells acted as negative control. The OD was measured (Microplate reader ELx800; BioTek, USA) and data was analyzed. All samples were tested in triplicate and repeated.

2.9. Virtual preparation of proteins and ligands

The interactions *S. monoica* derived compounds with caspase-3 and caspase-7 were elucidated by performing molecular docking using AutoDock 4.2 as described elsewhere (Al-Shabib et al., 2020). Briefly, the three-dimensional coordinates of caspase-3 (PDB Id: 2XYG) and caspase-7 (PDB Id: 3IBC) were retrieved from PDB RCSB database (www.rcsb.org). The proteins were pre-processed by removing water molecules or bound hetero atoms, if any, including addition of hydrogens and assigning Kollman charges. The structure of protein molecules was finally energy-minimized using Merck Molecular Force Field (MMFF). The 2D structures of all compounds were drawn in ChemDraw. All the compounds, including control ligands such as TQ8 (bound to Caspase-3 active site in the crystal structure) and Acetyl-YVAD-CHO (bound to Caspase-7 in the crystal structure) were prepared for docking by assigning bond orders and angles. For all structures, Gasteiger partial charges were defined and the energies of were minimized using UFF (Universal Force Field).

2.10. Molecular docking

Grids around the active site of the targets were defined by selecting the amino acid residues that interacted with the bound ligand. For caspase-3 and Caspase-7, grid boxes 33.3 × 28.8 × 28.3 Å and 25.1 × 34.5 × 29.8 Å, centered at 36.4 × 37.4 × 31.5 Å and 49.8 × -26.4 × -2.3 Å with 0.375 Å, respectively were used for molecular docking in AutoDcok 4.2 (Morris et al., 2009). The van der Waals' and electrostatic parameters were calculated with the help of distance-dependent dielectric function. Docking was performed using Lamarck Genetic Algorithm (LGA) and Solis-Wets local search methods. A total of 10 docking runs were performed with 2.5×10^6 energy calculations for each. The population size (150), translational step (0.2), quaternions (5.0) and torsions (5.0) were set. The docking affinity (K_b) of ligands for proteins was estimated from docking energy (ΔG) using the equation: $\Delta G = -RT\ln K_b$ (Boltzmann gas constant, R = 1.987 cal/mol/K and temperature, T = 298 K). The molecular docking procedure generated several low energy binding poses for each ligand, of which the complex with the lowest energy was selected for the analysis.

2.11. Statistical analysis

All data in triplicate were presented as mean ± SD and analyzed using one-way analysis of variance. Differences between two groups were compared using Student's *t*-test (SPSS software; Version 25; IBM, USA), and $p < 0.05$ was considered significant.

3. Results

3.1. Endothelial cell proliferative activities of S. Monoica derived compounds

All tested compounds (NSQ, SND, AES, NDX, ABN and BMN) were non-toxic to HUVEC cells even at the highest dose (50 µg/ml) in line with microscopic observations (data not shown). Our MTT assay showed dose-dependent cell proliferative activities of all compounds. Of these, SND (53.7%), NSQ (51.4%) and NDX (48%) exhibited relatively higher effects than AES (46.2%), ABN (44.8%) and BMN (42.8%) at 25 µg/ml in relation to untreated control (Fig. 2). There were no significant changes in growth enhancement at 50 µg/ml dose.

3.2. Attenuation of oxidative cell damage by S. Monoica derived compounds

Based on the promising cell proliferative activities, all six compounds (25 and 50 µg/ml, each) were evaluated for their cytoprotective potential against DCF-induced oxidative damage in HUVEC cells. As shown by MTT assay, cell viability was restored (in the order) by SND (80.5%), NSQ (80%), NDX (77%), ABN (75.2%), AES (72.5%) and BMN (71.35%) at 25 µg/ml dose. Notably, SND and NSQ showed the best activities as compared to the reference drug AG (88.5%) through attenuation of DCF (Fig. 3). Treatment with

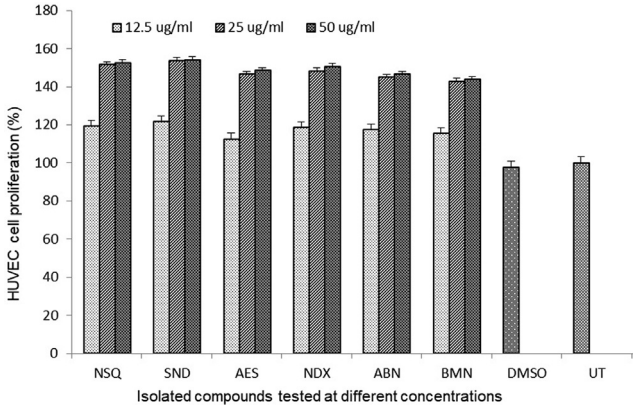

Fig. 2. Cell proliferative (MTT) assay showing dose-dependent growth stimulatory activity of *Suaeda monoica* derived new compounds (12.5, 25 and 50 μg/ml): norsesquaterpenol (NSQ), suaedanortriterpenedione (SND), aromatic monoterpenic ester (AES), norditerpenic xyloside (NDX), alkylated β-naphthol (ABN) and β-methoxy naphthalene (BMN) in cultured human endothelial cells (HUVEC). UT: untreated. Values on Y-axis: means of three determinations. All samples in triplicate were test-repeated twice.

50 mg/ml dose however, did not show significant enhancement in their activities.

3.3. Reversal of apoptotic cell death by S. Monoica derived compounds

Further, when tested against MGO-induced apoptosis, HUVEC cell death were reversed and rejuvenated (in the order) by SND (82.3%), NSQ (78.3%), NDX (79.8%), AES (74%), ABN (72.6%) and BMN (69.8%) at 25 μg/ml dose. Notably, SND, NSQ and NDX showed the best activities as compared to the reference drug AG activity (89.4%) (Fig. 4). The 50 mg/ml dose did not show significant additive effect.

3.4. S. monoica derived compounds effectively down regulated cellular caspase-3/7

Further insight into the anti-apoptotic mechanism of the three most active terpenic compounds (25 μg/ml) showed modulation of caspase-3/7 activities in both DCF and MGO treated HUVEC cells. DCF and MGO induced cellular caspases by 76.3% and 81.3%, respectively (Fig. 5). NSQ, NDX and SND efficiently down regulated caspase-3/7 expressions by 44.3%, 42.2% and 39.4%, respectively against DCF, whereas by 46.2%, 43.5% and 42.5%, respectively against MGO (Fig. 5). The reference drug AG downregulated caspase-3/7 by 56.2% and 54.7% through attenuation of DCF and MGO, respectively.

3.5. Interaction between caspase-3 and S. Monoica derived compounds

Our molecular docking analysis revealed that all the compounds were able to bind to the active site of caspase-3 (Fig. 6, IA), and their binding energy and corresponding binding affinity towards caspase-3 were estimated (Table 1). The interaction between caspase-3 and TQ8 (ligand control) suggested involvement of three hydrogen bonds with Arg207, and two hydrophobic interactions with Trp206. Some other residues such as Ser65, Tyr204, Ser205, Asn208, Ser209, and Phe250 formed van der Waals' interactions (Fig. 6, IB; Table 2). The binding energy and affinity of TQ8 and caspase-3 complex were estimated to be -5.8 kcal mol^{-1} and 1.79×10^4 M^{-1}, respectively (Table 1).

Alkylated β-naphthol formed a stable complex with caspase-3 mainly through hydrogen bonding with Arg207 and Ser251, including other hydrophobic interactions (Fig. 6, IC; Table 2). The complex was further stabilized by van der Waals' interactions with Tyr204, Ser205, Trp206, Phe252, and Asp253. The binding energy and affinity of the complex were estimated to be -6.1 kcal mol^{-1} and 2.98×10^4 M^{-1}, respectively (Table 1).

Aromatic monoterpenic ester and caspase-3 complex was stabilized by an electrostatic interaction (Pi-Cation) with His121 and three hydrogen bonds with His121, Cys163 and Glu123. Some other residues such as Thr62, Gly122, Gly165, and Thr166 formed van der Waals' interactions (Fig. 6 ID; Table 2). The docking energy and affinity of the complex were estimated to be -5.5 kcal mol^{-1} and 1.08×10^4 M^{-1}, respectively (Table 1).

β-methoxy naphthalene formed a stable complex with caspase-3 mainly through hydrogen bonding with Tyr204 and Arg207 as well as hydrophobic interactions (Fig. 6, IIA; Table 2). The complex was further stabilized by van der Waals' interactions with Asp253.

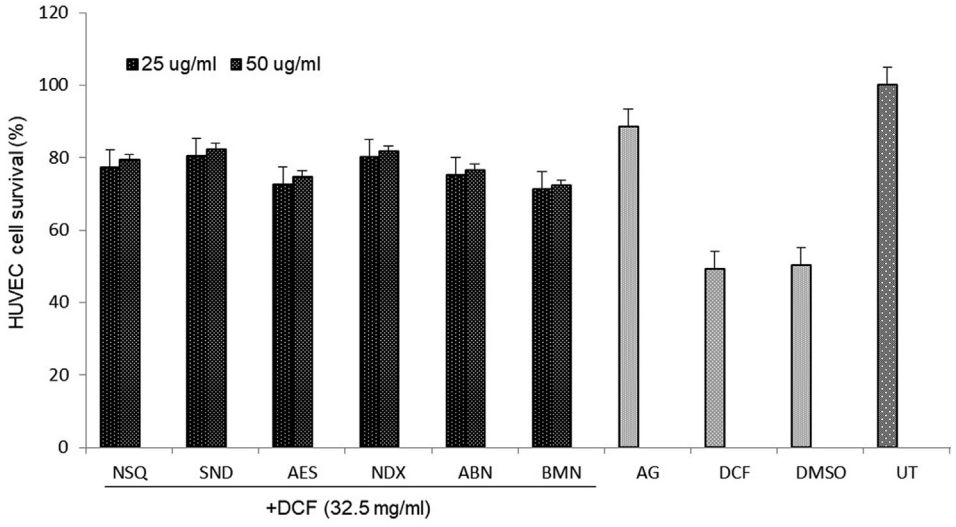

Fig. 3. Cell proliferative (MTT) assay showing cytoprotective activity of *Suaeda monoica* derived new compounds (25 and 50 μg/ml): norsesquaterpenol (NSQ), suaedanortriterpenedione (SND), aromatic monoterpenic ester (AES), norditerpenic xyloside (NDX), alkylated β-naphthol (ABN) and β-methoxy naphthalene (BMN) against dichlorofluorescin (DCF; 32.5 ug/ml) induced oxidative stress in cultured human endothelial cells (HUVEC). DMSO: vehicle control; UT: un-treated control. Values on Y-axis: means of three determinations. All samples in triplicate were test-repeated twice.

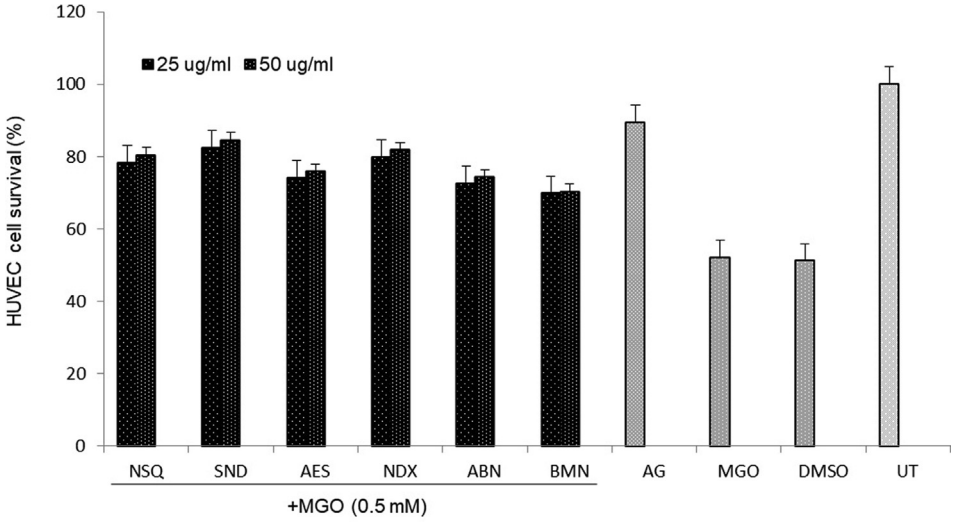

Fig. 4. Cell proliferative (MTT) assay showing cytoprotective activity of *Suaeda monoica* derived new compounds (25 and 50 μg/ml): norsesquaterpenol (NSQ), suaedanortriterpenedione (SND), aromatic monoterpenic ester (AES), norditerpenic xyloside (NDX), alkylated β-naphthol (ABN) and β-methoxy naphthalene (BMN) against Methylglyoxal (MGO; 0.05 mM) triggered apoptosis in cultured human endothelial cells (HUVEC). DMSO: vehicle control; UT: un-treated control. Values on Y-axis: means of three determinations. All samples in triplicate were test-repeated twice.

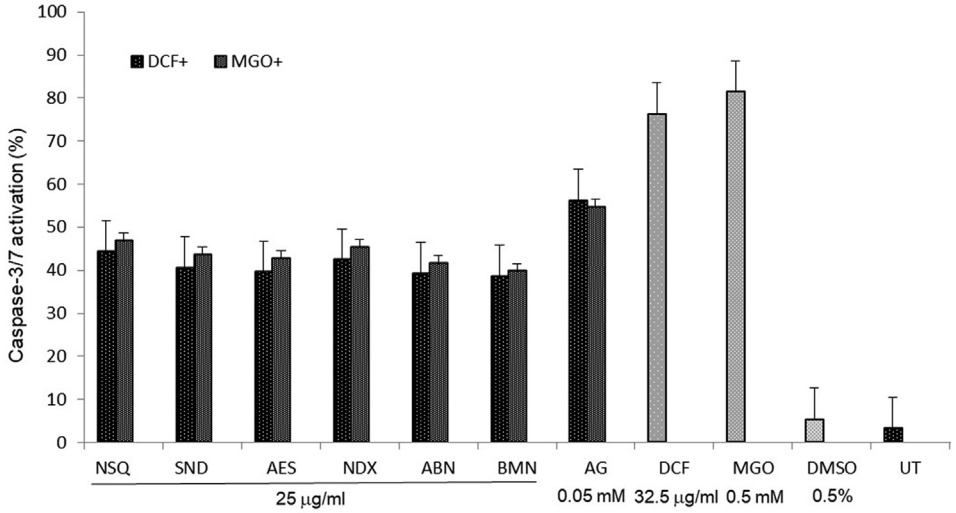

Fig. 5. The anti-apoptotic assay showing inhibition of dichlorofluorescin (DCF; 32.5 μg/ml) and methylglyoxal (MGO; 0.05 mM) induced cellular caspase-3/7 expressions by *Suaeda monoica* derived new compounds (25 μg/ml): suaedanortriterpenedione (SND), norsesquaterpenol (NSQ) and norditerpenic xyloside (NDX) in cultured human endothelial cells (HUVEC). DMSO: vehicle control; UT: un-treated control. Values on Y-axis: means of three determinations. All samples in triplicate were test-repeated twice.

The estimated binding energy and affinity of the complex were −5.8 kcal mol^{-1} and 1.79 × 10^4 M^{-1} respectively (Table 1).

Norditerpenic xyloside and caspase-3 complex was formed through three hydrogen bonds involving Arg207, Cys163 and Tyr204 as well as six hydrophobic interactions with Met61, His121, Phe128 and Cys163. Some other residues also formed van der Waals' interactions (Fig. 6, IIB; Table 2). The docking energy and affinity of the complex were estimated to be −6.6 kcal mol^{-1} and 6.93 × 10^4 M^{-1}, respectively (Table 1).

Norsesquaterpenol formed a stable complex with caspase-3 mainly through hydrophobic interactions with Phe256 (Fig. 6, IIC; Table 2). The complex was further stabilized by van der Waals' interactions involving Tyr204, Trp206, Arg207, Asn208, Ser209, Lys210, Phe250, Ser251 and Asp253. The calculated binding energy and affinity of the complex were −7.4 kcal mol^{-1} and 2.68 × 10^5 M^{-1}, respectively (Table 1).

Suaedanortriterpenedione and caspase-3 formed complex via two hydrogen bonds involving Ser209 and Phe250 as well as through hydrophobic interactions with Trp206, Arg207, Phe252 and Phe256. Some residues like Tyr204, Asn208 and Ser251 also showed van der Waals' interactions (Fig. 6, IID; Table 2). The docking energy and affinity of the complex were estimated to be −5.5 kcal mol^{-1} and 1.08 × 10^4 M^{-1}, respectively (Table 1).

3.6. Interaction between caspase-7 and S. Monoica derived compounds

All tested compounds showed good interaction with caspase-7 active site (Fig. 7, IA), and their binding energy and corresponding binding affinity towards caspase-7 were calculated (Table 1). The interaction between Acetyl-YVAD-CHO (ligand control) and caspase-7 suggested the involvement of hydrogen bonds with Arg233, Gln276 and His272. Some other residues such as Ser231,

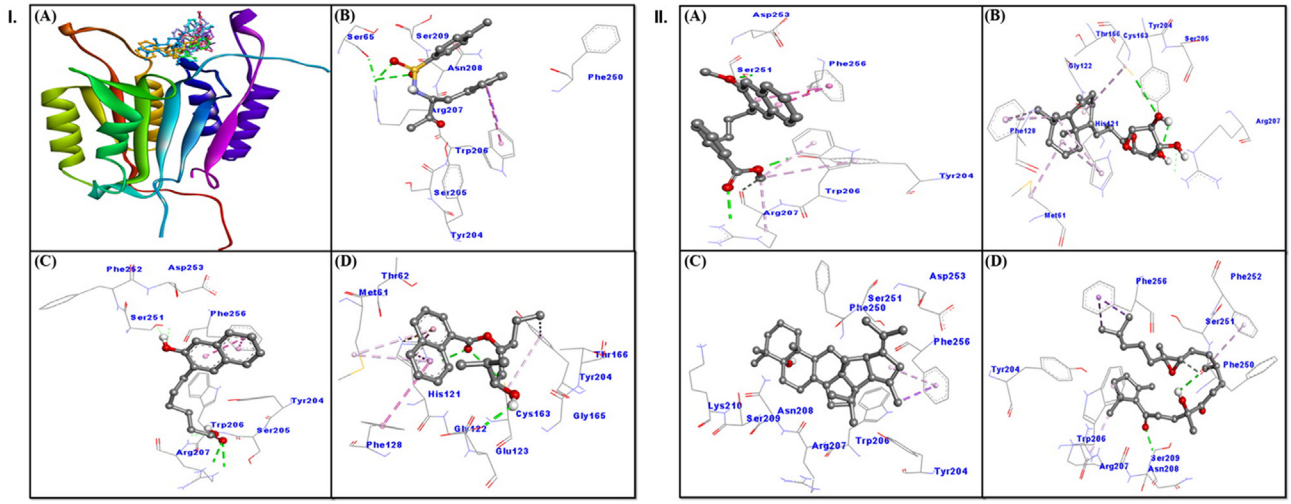

Fig. 6. The *in silico* molecular docking analysis showing interaction of caspase-3 with *Suaeda monoica* derived compounds. Panel I: (A) all compounds, (B) ligand control TQ8, (C) Alkylated β-naphthol, (D) Aromatic monoterpenic; Panel II: (A) β-methoxy naphthalene, (B) Norditerpenic xyloside, (C) Norsesquaterpenol, (D) Suaedanortriterpenedione.

Table 1
Molecular docking analysis of complexes formed by *S. monoica* derived compounds with caspase-3 and caspase-7.

Ligands	Caspase-3		Caspase-7	
	Binding energy (kcal mol^{-1})	Binding affinity (M^{-1})	Binding energy (kcal mol^{-1})	Binding affinity (M^{-1})
Ligand control*	−5.8	1.79×10^4	−9.6	1.10×10^7
Norsesquaterpenol	−7.4	2.68×10^5	−8.0	7.37×10^5
Suaedanortriterpenedione	−5.5	1.08×10^4	−6.2	3.53×10^4
Aromatic monoterpenic ester	−5.5	1.08×10^4	−5.7	1.52×10^4
Norditerpenic xyloside	−6.6	6.93×10^4	−7.6	3.75×10^5
Alkylated β-naphthol	−6.1	2.98×10^4	−6.6	6.93×10^4
β-methoxy naphthalene	−5.8	1.79×10^4	−6.3	4.18×10^4

*Ligand controls: TQ8 (N-[(2S)-4-chloro-3-oxo-1-phenyl-butan-2-yl]-4-methyl-benzenesulfonamide) for caspase- 3 and Acetyl-YVAD-CHO for caspase-7.

Trp232, Ser234, Pro235, Arg237, Trp240, Phe273, Glu274, Ser275, Ser277 and Phe282 formed van der Waals' interactions (Fig. 7, IB; Table 3). The docking energy and docking affinity of Acetyl-YVAD-CHO for caspase-7 were estimated to be −9.6 kcal mol^{-1} and 1.10×10^7 M^{-1}, respectively (Table 1).

Alkylated β-naphthol formed a stable complex with caspase-7 mainly through hydrogen bonding which involved Arg87, His144 and Arg233, wherein His114 also formed a carbon-hydrogen bond (Fig. 7, IC; Table 3). The ABN-Caspase 7 complex was further stabilized by van der Waals' interactions with SER143, GLY145, GLN184, ALA185, CYS186, SER231, TRP232, SER277, and PHE282. The binding energy of ABN-Caspase 7 complex formation was estimated to be −6.6 kcal mol^{-1} while the binding affinity was determined to be 6.93×10^4 M^{-1} (Table 1).

Aromatic monoterpenic ester and caspase-7 complex was stabilized by a hydrogen bond involving Cys186, and hydrophobic interactions with Tyr230 and Trp232. Residues such as Ser231, Arg233, Ser277 and Phe282 formed van der Waals' interactions (Fig. 7, ID; Table 3), Table 3). The estimated binding energy and docking affinity of the complex were −5.7 kcal mol^{-1} and 1.52×10^4 M^{-1}, respectively (Table 1).

β-methoxy naphthalene formed a stable complex with caspase-7 mainly through a carbon- hydrogen bond involving His144 and hydrophobic interactions with Cys186, Tyr230 and Trp232 (Fig. 7, IIA; Table 3). The complex was further stabilized by van der Waals' interactions involving Met84, Ser231, Arg233, Ser277 and Phe282. The binding energy and affinity of the complex was estimated to be −6.3 kcal mol^{-1} and 4.18×10^4 M^{-1}, respectively (Table 1).

Norditerpenic xyloside and caspase-7 formed complex via two hydrogen bonds with Trp240 and Gln276 as well as. Through hydrophobic interactions involving Cys186, Tyr230 and Trp232 (Fig. 7, IIB; Table 3). Also, it showed van der Waals' interactions with Ser231, Arg233, Ser234, Arg237, Ser275 and Ser277. The calculated docking energy and affinity of the complex were −7.6 kcal mol^{-1} and 3.75×10^5 M^{-1}, respectively (Table 1).

Norsesquaterpenol formed a stable complex with caspase-7 mainly through hydrophobic interactions, involving Trp232, Pro235, Trp240 and others as well as one hydrogen bond with Gln276, (Fig. 7, IIC; Table 3). The complex was further stabilized by van der Waals' interactions with Val86, Arg233, Ser234, Arg237, Glu274, Ser275 and Ser277. The binding energy and affinity of the complex were −8.0 kcal mol^{-1} and 7.37×10^5 M^{-1}, respectively (Table 1).

Suaedanortriterpenedione and caspase-7 complex was formed with two hydrogen bonds involving Cys186 and Arg233 as well as hydrophobic interactions with Cys186, Tyr230, Trp232, Pro235, Trp240 and Phe282. Some residues such as Ser231, Ser275, Gln276 and Ser277 showed van der Waals' interactions (Fig. 7, IID; Table 3). The estimated docking energy and affinity of the complex were −6.2 kcal mol^{-1} and 3.53×10^4 M^{-1}, respectively (Table 1).

4. Discussions

Several natural or plants products are known to have cell proliferative and cytoprotective potential via anti-oxidative, anti-

Table 2
Molecular docking parameters for the interaction between caspase-3 and *S. monoica* derived compounds.

Ligands	Donor-Acceptor pair	Distance (Å)	Type of interaction	Van der Waals' interaction
Control*	ARG207:HN - LIG:O	1.8753	Conventional Hydrogen Bond	SER65, TYR204, SER205, ASN208, SER209, PHE250
	ARG207:HH11 - LIG:O	2.9212	Conventional Hydrogen Bond	
	ARG207:HH21 - LIG:O	2.2992	Conventional Hydrogen Bond	
	TRP206:CZ3 - LIG	3.6914	Hydrophobic (Pi-Sigma)	
	TRP206 - LIG	5.0512	Hydrophobic (Pi-Pi T-shaped)	
ABN	ARG207:HE - LIG:O	2.4690	Conventional Hydrogen Bond	TYR204, SER205, TRP206, PHE252, ASP253
	ARG207:HH22 - LIG:O	2.4750	Conventional Hydrogen Bond	
	ARG207:HN - LIG:O	2.4534	Conventional Hydrogen Bond	
	SER251:HG - LIG:O	2.4498	Conventional Hydrogen Bond	
	LIG:H - SER251:OG	1.8630	Conventional Hydrogen Bond	
	PHE256 - LIG	3.8742	Hydrophobic (Pi-Pi Stacked)	
	PHE256 - LIG	4.0116	Hydrophobic (Pi-Pi Stacked)	
AES	HIS121:HD1 - LIG:O	2.3773	Conventional Hydrogen Bond	THR62, GLY122, GLY165, THR166
	CYS163:SG - LIG:O	3.6886	Conventional Hydrogen Bond	
	LIG:H - GLU123:OE1	2.3259	Conventional Hydrogen Bond	
	HIS121:NE2 - LIG	4.3581	Electrostatic (Pi-Cation)	
	HIS121 - LIG	4.0199	Hydrophobic (Pi-Pi Stacked)	
	HIS121 - LIG	4.6979	Hydrophobic (Pi-Pi Stacked)	
	PHE128 - LIG	5.0433	Hydrophobic (Pi-Pi T-shaped)	
	TYR204 - LIG:C	4.9384	Hydrophobic (Pi-Alkyl)	
	LIG - MET61	5.3853	Hydrophobic (Pi-Alkyl)	
	LIG - MET61	4.9636	Hydrophobic (Pi-Alkyl)	
BMN	TYR204:HH - LIG:O	2.0032	Conventional Hydrogen Bond	ASP253
	ARG207:HH22 - LIG:O	2.4339	Conventional Hydrogen Bond	
	SER251:HG - LIG:O	2.3132	Conventional Hydrogen Bond	
	LIG:C - ARG207:O	3.5213	Carbon Hydrogen Bond	
	PHE256 - LIG	3.7981	Hydrophobic (Pi-Pi Stacked)	
	PHE256 - LIG	3.8563	Hydrophobic (Pi-Pi Stacked)	
	LIG:C - ARG207	4.5903	Hydrophobic (Alkyl)	
	TYR204 - LIG:C	5.3747	Hydrophobic (Pi-Alkyl)	
	TRP206 - LIG:C	5.0178	Hydrophobic (Pi-Alkyl)	
NDX	ARG207:HH22 - LIG:O	2.3814	Conventional Hydrogen Bond	GLY122, THR166, SER205
	CYS163:SG - LIG:O	3.4607	Conventional Hydrogen Bond	
	TYR204:HH - LIG:O	2.7000	Conventional Hydrogen Bond	
	MET61 - LIG	4.7801	Hydrophobic (Alkyl)	
	CYS163 - LIG	5.1548	Hydrophobic (Alkyl)	
	HIS121 - LIG	4.4606	Hydrophobic (Pi-Alkyl)	
	HIS121 - LIG:C	4.9783	Hydrophobic (Pi-Alkyl)	
	PHE128 - LIG:C	5.0270	Hydrophobic (Pi-Alkyl)	
	PHE128 - LIG:C	4.1657	Hydrophobic (Pi-Alkyl)	
NSQ	LIG:C - PHE256	3.5475	Hydrophobic (Pi-Sigma)	TYR204, TRP206, ARG207, ASN208, SER209, LYS210,
	PHE256 - LIG	4.4100	Hydrophobic (Pi-Alkyl)	PHE250, SER251, ASP253
SND	SER209:HN - LIG:O	2.2032	Conventional Hydrogen Bond	TYR204, ASN208, SER251
	LIG:H - PHE250:O	2.3776	Conventional Hydrogen Bond	
	LIG:C - PHE250:O	3.2851	Carbon Hydrogen Bond	
	LIG:C - PHE256	3.9312	Hydrophobic (Pi-Sigma)	
	LIG:C - PHE256	3.7106	Hydrophobic (Pi-Sigma)	
	LIG:C - ARG207	4.5144	Hydrophobic (Alkyl)	
	TRP206 - LIG:C	4.4890	Hydrophobic (Pi-Alkyl)	
	PHE252 - LIG:C	4.8691	Hydrophobic (Pi-Alkyl)	

*Chemically the control TQ8 is N-[(2S)-4-chloro-3-oxo-1-phenyl-butan-2-yl]-4-methyl-benzenesulfonamide.

inflammatory and tissue-rejuvenating/regenerative activities (Kong et al., 2004; Kim et al., 2013; Parvez et al., 2018; Parvez et al., 2019; Alqahtani et al., 2019; Parvez et al., 2020). Plant secondary metabolites have high chemical diversity and biochemical specificity, which often act more effectively than synthetic drugs (Ganesan, 2008). In the present study, *S. monoica* derived new four terpenes (a norsesquaterpenol, a monocyclic triterpenoid, an aromatic monoterpenic ester and a norditerpenic xyloside) and two phenols (an alkylated β-naphthol and a β-methoxy naphthalene) were studied for their cell proliferative and cytoprotective efficacies in cultured endothelial cells. Notably, we have used the non-cytotoxic optimal dose of 50 μg/ml for all tested compounds as compared to previously reported maximal non-cytotoxic concentrations of monoterpenes up to 60 μg/ml (Astani and Schnitzler, 2014).

Plant essential oils comprising of a diverse group of terpenes (monoterpenes and sesquiterpenes) and phenylpropanoids including carbohydrate, alcohol, ether, aldehyde and ketones are attributed to fragrance and flavor as well as a wide range of medicinal applications. Cellular accumulation of highly toxic reactive oxygen species (ROS) can damage lipids, proteins or nucleic acids, and normal cell growth and function leading to tissue damages (Opara and Rockway, 2006). In *in vitro* settings, DCF is generally used for estimating free–radical triggered oxidative stress (LeBel et al., 1992; Oyama et al., 1994; Rota et al., 1999). In cultured endothelial cells, its oxidation is suggested as a result of H_2O_2 dependent reactions involving cytochrome *c* and Fe^{2+} (Royall and Ischiropoulos, 1993; Carter et al., 1994). Here we demonstrate the maximal endothelial cell proliferation and cytoprotection by suaedanortriterpenedione, norsesquaterpenol and norditerpenic xyloside, whereas moderately by aromatic monoterpenic ester, alkylated β-naphthol and β-methoxy naphthalene via attenuation of DCF in line with our recent reports on other phytoproducts (Alqahtani et al., 2019; Parvez et al., 2020).

In hyperglycemia, the role of endogenous aldehydes and their end-products, including the highly reactive MGO is suggested as

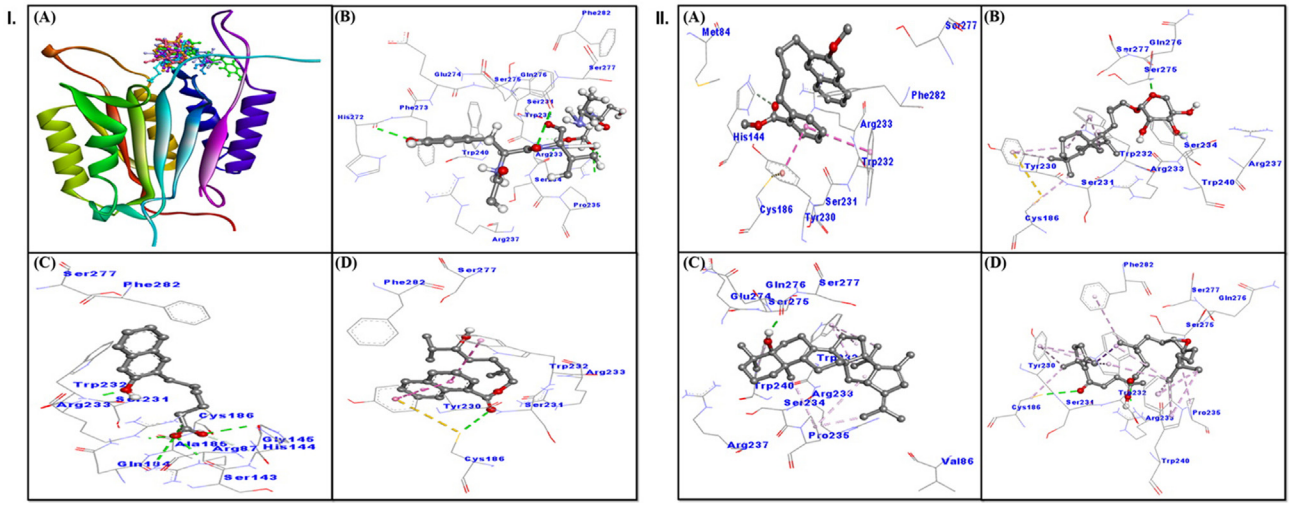

Fig. 7. The *in silico* molecular docking analysis showing interaction of caspase-7 with *Suaeda monoica* derived compounds. Panel I: (A) all compounds, (B) ligand control Acetyl-YVAD-CHO, (C) Alkylated β-naphthol, (D) Aromatic monoterpenic; Panel II: (A) β-methoxy naphthalene, (B) Norditerpenic xyloside, (C) Norsesquaterpenol, (D) Suaedanortriterpenedione.

Table 3
Molecular docking parameters for the interaction between caspase-7 and *S. monoica* derived compounds.

Ligand	Donor-Acceptor pair	Distance (Å)	Type of interaction	Van der Waals's interaction
Control*	ARG233:HN - LIG:O	2.0867	Conventional Hydrogen Bond	SER231, TRP232, SER234, PRO235, ARG237, TRP240,
	ARG233:HH11 - LIG:O	2.7924	Conventional Hydrogen Bond	PHE273, GLU274, SER275, SER277, PHE282
	ARG233:HH21 - LIG:O	2.5474	Conventional Hydrogen Bond	
	LIG:O – GLN276	3.0801	Conventional Hydrogen Bond	
	LIG:H - HIS272:O	2.5836	Conventional Hydrogen Bond	
	LIG:HO - ARG233:O	2.7121	Conventional Hydrogen Bond	
ABN	ARG87:HE - LIG:O	2.3632	Conventional Hydrogen Bond	SER143, GLY145, GLN184, ALA185, CYS186,
	ARG87:HH22 - LIG:O	2.8463	Conventional Hydrogen Bond	SER231, TRP232, SER277, PHE282
	HIS144:HD1 - LIG:O	2.6366	Conventional Hydrogen Bond	
	ARG233:HN - LIG:O	1.9248	Conventional Hydrogen Bond	
	ARG233:HE - LIG:O	2.1267	Conventional Hydrogen Bond	
	ARG233:HH22 - LIG:O	2.1997	Conventional Hydrogen Bond	
	HIS144:CA - LIG:O	3.3939	Carbon Hydrogen Bond	
AES	CYS186:SG - LIG:O	3.5904	Conventional Hydrogen Bond	SER231, ARG233, SER277, PHE282
	CYS186:SG - TYR230	4.6432	Hydrophobic (Pi-Sulfur)	
	TYR230 - LIG	4.2061	Hydrophobic (Pi-Pi Stacked)	
	TYR230 - LIG	4.5641	Hydrophobic (Pi-Pi Stacked)	
	TRP232 - LIG	4.8124	Hydrophobic (Pi-Pi T-shaped)	
BMN	HIS144:CE1 - LIG:O	3.6982	Carbon Hydrogen Bond	MET84, SER231, ARG233, SER277, PHE282
	TYR230 - LIG	3.7578	Hydrophobic (Pi-Pi Stacked)	
	TRP232 - LIG	5.0180	Hydrophobic (Pi-Pi T-shaped)	
NDX	TRP240:HE1 - LIG:O	2.1034	Conventional Hydrogen Bond	SER231, ARG233, SER234, ARG237, SER275, SER277
	GLN276:HN - LIG:O	2.0006	Conventional Hydrogen Bond	
	LIG:C - CYS186	4.6176	Hydrophobic (Alkyl)	
	TYR230 - LIG	4.6001	Hydrophobic (Pi-Alkyl)	
	TYR230 - LIG:C	4.7870	Hydrophobic (Pi-Alkyl)	
	TRP232 - LIG:C	4.9544	Hydrophobic (Pi-Alkyl)	
	TRP232 - LIG	4.6991	Hydrophobic (Pi-Alkyl)	
	TRP232 - LIG:C	4.4321	Hydrophobic (Pi-Alkyl)	
NSQ	LIG:H - GLN276:O	1.7762	Conventional Hydrogen Bond	VAL86, ARG233, SER234, ARG237,
	PRO235 - LIG	5.4848	Hydrophobic (Alkyl)	GLU274, SER275, SER277
	LIG:C - PRO235	4.7898	Hydrophobic (Alkyl)	
	LIG:C - PRO235	3.5114	Hydrophobic (Alkyl)	
	TRP232 - LIG	5.3563	Hydrophobic (Pi-Alkyl)	
	TRP232 - LIG:C	4.8321	Hydrophobic (Pi-Alkyl)	
	TRP232 - LIG:C	4.9250	Hydrophobic (Pi-Alkyl)	
	TRP240 - LIG:C	4.5652	Hydrophobic (Pi-Alkyl)	
	TRP240 - LIG:C	5.3680	Hydrophobic (Pi-Alkyl)	
SND	CYS186:SG - LIG:O	3.2926	Conventional Hydrogen Bond	SER231, SER275, GLN276, SER277
	ARG233:HN - LIG:O	2.1417	Conventional Hydrogen Bond	
	LIG:C - TRP232	3.5878	Hydrophobic (Pi-Sigma)	
	LIG:C - CYS186	4.8621	Hydrophobic (Alkyl)	
	LIG:C - PRO235	4.4650	Hydrophobic (Alkyl)	
	TYR230 - LIG	3.8562	Hydrophobic (Pi-Alkyl)	

(*continued on next page*)

Table 3 (*continued*)

Ligand	Donor-Acceptor pair	Distance (Å)	Type of interaction	Van der Waals's interaction
	TYR230 - LIG:C	4.6311	Hydrophobic (Pi-Alkyl)	
	TYR230 - LIG:C	4.5072	Hydrophobic (Pi-Alkyl)	
	TRP232 - LIG:C	4.3383	Hydrophobic (Pi-Alkyl)	
	TRP232 - LIG:C	5.1841	Hydrophobic (Pi-Alkyl)	
	TRP232 - LIG:C	5.0696	Hydrophobic (Pi-Alkyl)	
	TRP240 - LIG:C	5.0866	Hydrophobic (Pi-Alkyl)	
	TRP240 - LIG:C	4.5228	Hydrophobic (Pi-Alkyl)	
	TRP240 - LIG:C	5.1945	Hydrophobic (Pi-Alkyl)	
	TRP240 - LIG:C	4.7176	Hydrophobic (Pi-Alkyl)	
	PHE282 - LIG:C	5.3566	Hydrophobic (Pi-Alkyl)	

* The chemical nature of Caspase 7 control ligand (peptide based inhibitor) is Acetyl-YVAD-CHO.

a prime inducer of vascular endothelial cell damage via oxidative stress and apoptosis (Bourajjaj et al., 2003; Kim et al., 2004; Phalitakul et al., 2013; Figarola et al., 2014). Recently, significant reversal of MGO induced HUVEC cell apoptosis by pyrrophenone has been demonstrated (Ravikumar et al., 2010; Yuan et al., 2017). In addition, we have also reported promising cytoprotection of HUVEC cells against MGO by rhuspartin (Alqahtani et al., 2019) and oncoglabrinol C (Parvez et al., 2020). In line with this, we demonstrate the maximal HUVEC cell proliferation and cytoprotection by suaedanortriterpenedione, norsesquaterpenol and norditerpenic xyloside, whereas moderately by aromatic monoterpenic ester, alkylated β-naphthol and β-methoxy naphthalene through amelioration of MGO.

Caspases belong to cysteine-aspartate proteases, which play crucial roles in maintaining cellular homeostasis by inducing apoptotic cell death and tissue inflammation (Kumar, 2006). All caspases are synthesized as inactive enzymes where activation of effector caspase-3 or 7 is performed by the initiator caspase-9 that itself is autoactivated under oxidative or apoptotic conditions (Boatright and Salvesen, 2003; Shi, 2000). Therefore, the therapeutic intervention that could inhibit caspase expressions in acute and chronic diseases are very much desirable. To have an insight into the plausible underlying mechanisms involved in anti-oxidative and anti-apoptotic salutations, suaedanortriterpenedione, norsesquaterpenol and norditerpenic xyloside, the most active terpenes were further assessed for caspase-3/7 modulating potential. Our data showed that the three terpenes effectively downregulated DCF and MGO activated caspase-3/7 expressions in HUVEC cells, endorsing our previous observation (Alqahtani et al., 2019; Parvez et al., 2020). Furthermore, *in silico* docking results also confirmed that suaedanortriterpenedione, norsesquaterpenol and norditerpenic xyloside as well the control ligands (TQ8 and Acetyl-YVAD-CHO) interacted with key substrate-binding and catalytic residues of caspase-3 and 7. The complexex between caspase-37 and the phytocompounds were stabilized by hydrogen bondings, hydrophobic interactions and van der Waals' interactions. Interestingly, some amino acid residues of caspase-3 were commonly involved in the interaction with TQ8 as well as suaedanortriterpenedione (Tyr204, Trp206, Arg207, Asn208, Ser209, and Phe250), norsesquaterpenol (Tyr204, Trp206, Arg207, Asn208, Ser209, Phe250) and norditerpenic xyloside (Tyr204, Ser205, Arg207, and Phe250). Similarly, the amino acid residues Ser231, Trp232, Arg233, Pro235, Trp240, Ser275, Gln276, Ser277 and Phe282 of caspase-7 were involved in the interaction with Acetyl-YVAD-CHO and suaedanortriterpenedione. For norsesquaterpenol, the interacting residues were Trp232, Arg233, Ser234, Pro235, Arg237, Trp240, Glu274, Ser275, and Ser277, whereas for norditerpenic xyloside, those were Ser231, Trp232, Arg233, Ser234, Arg237, Trp240, Ser275, Gln276 and Ser277. This is in line with our previous study where Oncoglabrinol C, a flavan isolated from *Oncocalyx glabratus* strongly interacted with the substrate binding sites of caspase 3/7, and suggested inhibition of their catalytic acivities (Parvez et al., 2020).

5. Conclusion

Our data for the first time demonstrate *in vitro* cell proliferative, anti-oxidative and anti-apoptotic efficacies of *Suaeda monoica* derived novel terpenes *viz.*, suaedanortriterpenedione, normonisesquaterpenol, and norditerpenic xyloside in human primary endothelial cells. This warrants their further molecular and pharmacological assessment as vascular cell protective as well as tissue-rejuvenating therapeutics, especially in hyperglycemic conditions.

Declaration of Competing Interest

The authors declare that they have no known competing financial interests or personal relationships that could have appeared to influence the work reported in this paper.

Acknowledgement

The authors thankfully acknowledge the Researchers Supporting Project (RSP-2021/379), King Saud University, Riyadh for funding this work.

References

AlSaid, M.S., Siddiqui, N.A., Mukhair, M.A., Parvez, M.K., Alam, P., Ali, M., Haque, A., 2017. A novel monocyclic triterpenoid and a norsesquaterpenol from the aerial parts of *Suaeda monoica* Forssk. ex J. F. Gmel with cell proliferative potential. Saudi Pharm. J. 25, 1005–1010.

Alqahtani, A.S., Abdel-mageed, W.M., Shahat, A.A., Parvez, M.K., Al-Dosari, M.S., Malik, A., Abdel-Kader, M.S., Alsaid, M.S., 2019. Proanthocyanidins from the stem bark of *Rhus tripartita* and their amelioration of methylglyoxal-induced apoptosis of endothelial cells. J. Food Drug Anal. 27, 358–365.

Al-Shabib, N.A,, Khan, J.M., Malik, A., Rehman, M.T., AlAjmi. M.F., Husain, F.M., Ahmad, A. Sen P., 2020. Investigating the effect of food additive azo dye "tartrazine" on BLG fibrillation under in-vitro condition. A biophysical and molecular docking study. J. King Saud Univ.–Sci. 32, 2034-2040.

Arbab, A.H., Parvez, M.K., Al-Dosari, M.S., Al-Rehaily, A.J., Ibrahim, K.E., Alam, P., AlSaid, M.S., Rafatullah, S., 2016. Therapeutic efficacy of ethanolic extract of *Aerva Javanica* aerial parts in the amelioration of CCl_4-induced hepatotoxicty and oxidative damage in rats. Food Nutr. Res. 60, 30864.

Astani, A., Schnitzler, P., 2014. Antiviral activity of monoterpenes beta-pinene and limonene against herpes simplex virus in vitro. Iranian J. Microbiol. 6, 149–155.

Boatright, K.M., Salvesen, G,S., 2003. Mechanisms of caspase activation. Curr. Opin. Cell Biol. 15, 725-731.

Bourajjaj, M., Stehouwer, C.D., van Hinsbergh, V.W., Schalkwijk, C.G., 2003. Role of methylglyoxal adducts in the development of vascular complications in diabetes mellitus. Biochem. Soc. Trans. 31, 1400–1402.

Carter, W.O., Narayanan, P.K., Robinson, J.P., 1994. Intracellular hydrogen peroxide and superoxide anion detection in endothelial cells. J. Leuk. Biol. 55, 253–258.

Choy, J.C., Granvilleab, D.J., Hunt, D.W.C., McManus, B.M., 2001. Endothelial cell apoptosis: biochemical characteristics and potential implications for atherosclerosis. J. Mol. Cell. Cardiol. 33, 1673–1690.

Figarola, J.L., Singhal, J., Rahbar, S., Awasthi, S., Singha,l S.S., 2014. LR-90 prevents methylglyoxal-induced oxidative stress and apoptosis in human endothelial cells. Apoptosis. 19, 776-788.
Ganesan, A., 2008. The impact of natural products upon modern drug discovery. Curr. Opin Chem. Biol. 12, 306–317.
Kim, J., Son, J.W., Lee, J.A., Oh, Y.S., Shinn, S.H., 2004. Methylglyoxal induces apoptosis mediated by reactive oxygen species in bovine retinal pericytes. J. Korean Med. Sci. 19, 95–100.
Kim, D.R., Kim, H.Y., Park, J.K., Park, S.K., Chang, M.S., Jeon, J.Y., 2013. Aconiti lateralis preparata radix activates the proliferation of mouse bone marrow mesenchymal stem cells and induces osteogenic lineage differentiation through the bone morphogenetic protein-2/smad-dependent runx2 pathway. Evid. Based Compl. Alter. Med. 2013, 86741.
Kong, X., Hu, Y., Rui, R., Wang, D., Li, X., 2004. Effects of Chinese herbal medicinal ingredients on peripheral lymphocyte proliferation and serum antibody titer after vaccination in chicken. Intl. Immunopharmacol. 4, 975–982.
Kathiresan, K., Ramanathan, T., 1997. Medicinal Plants of Parangipettai Coast. India, Annamalai University, Tamil Nadu, pp. 72–76.
Kokpal, V., Miles, D.H., Payne, A.M., Chittarwong, V., 1990. Chemical constituents and bioactive compounds from mangrove plants. Stud. Nat. Prod. Chem. 7, 175–199.
Kumar, S., 2006. Caspase function in programmed cell death. Cell Death Differen. 14, 32–43.
Lakshmanan, G., Rajeshkannan, C., Kavitha, A., Mekala, B., Kamaladevi, N., 2013. Preliminary screening of biologically active constituents of *Suaeda monoica* and *Sesuvium portulacastrum* from palayakayal mangrove forest of Tamilnadu. J. Pharmacog. Phytochem. 2, 149–152.
Lakshmi, K.P., Narsimha Rao, G.M., 2013. Antimicrobial activity of *Suaeda monoica* (Forsst ex Geml) against Human and plant pathogens. Res. J. Pharm. Biol. Chem. Sci. 4, 680–685.
LeBel, C.P., Ischiropoulos, H., Bondy, S.C., 1992. Evaluation of the probe 2′,7′-dichlorofluorescin as an indicator of reactive oxygen species formation and oxidative stress. Chem. Res. Toxicol. 5, 227–231.
Morris, G.M., Huey, R., Lindstrom, W., Sanner, M.F., Belew, R.K., Goodsell, D.S., Olson, A.J., 2009. Autodock4 and AutoDockTools4: automated docking with selective receptor flexiblity. J. Comput. Chem. 16, 2785–2791.
Muthazhagan, K., Thirunavukkarasu, P., Ramanathan, T., Kannan, D., 2014. Studies on phytochemical screening, antimicrobial and antiradical scavenging effect of a coastal salt mash plant *Suaeda monoica*. Res. J. Phytochem. 8, 102–111.
Opara, E.C., Rockway, S.W., 2006. Antioxidants and micronutrients. Dis, Mon. 52, 151-63.
Oyama, Y., Hayashi, A., Ueha, T., Maekawa, K., 1994. Characterization of 2′,7′-dichlorofluorescin fluorescence in dissociated mammalian brain neurons: estimation on intracellular content of hydrogen peroxide. Brain Res. 635, 113–117.
Parvez, M.K., Arbab, A.H., Al-Dosari, M.S., Al-Rehaily, A.J., Alam, P., Ibrahim, K.E., AlSaid, M.S., Rafatullah, S., 2018. Protective effect of *Atriplex suberecta* extract against oxidative and apoptotic hepatotoxicty. Exp. Therap. Med. 15, 3883–3891.
Parvez, M.K., Al-Dosari, M.S., Arbab, A.H., Alam, P., Alsaid, M.S., Khan, A.A., 2019. Hepatoprotective efficacy of *Solanum surattense* extract against chemical–induced oxidative and apoptotic injury in rats. BMC Compl. Alter. Med. 19, 155–162.
Parvez, M.K., Al-Dosari., M.S., Ahmed. S., Rehman, M.T., Al-Rehaily, A.J., 2020. Oncoglabrinol C, a new flavan from Oncocalyx glabratus protects human endothelial cells against oxidative and apoptotic damages and modulated hepatic CYP3A4 activity. Saudi Pharm. J. 28, 646-656.
Phalitakul, S., Okada, M., Hara, Y., Yamawaki, H., 2013. Vaspin prevents methylglyoxal-induced apoptosis in human vascular endothelial cells by inhibiting reactive oxygen species generation. Acta Physiol. (Oxford) 209, 212–219.
Ravikumar, S., Gnanadesigan, M., Serebiah, J., Inbaneson, S.J., 2010. Hepatoprotective effect of an Indian salt marsh herb *Suaeda monoica* Forrsk ex. Gmel against concanavalin-A induced toxicity in rats. Life Sci. Med. Res. 2, 1–9.
Rota, C., Chignell, C.F., Mason, R.P., 1999. Evidence for free radical formation during the oxidation of 2'-7'-dichlorofluorescin to the fluorescent dye 2'-7'-dichlorofluorescein by horseradish peroxidase: possible implications for oxidative stress measurements. Free Rad. Biol. Med. 27, 873–881.
Royall, J.A., Ischiropoulos, H., 1993. Evaluation of 2′,7′-dichlorofluorescin and dihydro-rhodamine 123 as fluorescent probes for intracellular H_2O_2 in cultured endothelial cells. Arch. Biochem. Biophys. 302, 348–355.
Shahat, A.A., Alsaid, M.S., Rafatullah, S., Al-Sohaibani, M.O., Parvez, M.K., Al-Dosari, M.S., Exarchou, V., Pieters, L., 2016. Treatment with *Rhus tripartita* extract curtails isoproterenol-elicited cardiotoxicity and oxidative stress in rats. BMC Compl. Alter. Med. 2016, 351.
Shi, Y., 2000. Caspase activation, inhibition, and reactivation: A mechanistic view. Protein Sci. 13, 1979–1987.
Siddiqui, N.A., Mothana, R.A., Al-Said, M.S., Parvez, M.K., Alam, P., Rehman, M.T., Ali, M., Alajmi, M.F., Al-Dosari, M.S., Al-Rehaily, A.J., Khalid, J.M., 2020. Cell proliferation activity delineated by molecular docking of four new compounds isolated from *Suaeda monoica* Forssk. ex. J.F. Gmel (aerial parts). Saudi Pharm. J. 28, 172–186.
Tanaka, R., Tsujimoto, K., In, Y., Matsunaga, S., 1997. New Methoxytriterpene Dione from the cuticle of *Picea jezoensis* var. jezoensis. J. Nat. Prod. 60, 319–322.
Thornalley, P.J., Rabbani, N., 2014. Assay of methylglyoxal and glyoxal and control of peroxidase interference. Biochem. Soc. Trans. 42, 504–510.
Yuan, J., Zhu, C., Hong, Y., Sun, Z., Fang, X., Wu, B., Li, S., 2017. The role of cPLA2 in Methylglyoxal-induced cell apoptosis of HUVECs. Toxicol. Appl. Pharmacol. 23, 44–52.
Vander Jagt, D.L., Hunsaker, L.A., 2003. Methylglyoxal metabolism and diabetic complications: roles of aldose reductase, glyoxalase-I, betaine aldehyde dehydrogenase and 2-oxoaldehyde dehydrogenase. Chem. Biol. Interact. 143, 341–351.